Chemical Patterns from Surface Grafted Resists for Directed Assembly of Block Copolymers

Eungnak Han,[†,‡] Myungwoong Kim,[†] and Padma Gopalan*

Department of Materials Science and Engineering, University of Wisconsin-Madison, Madison, Wisconsin 53706, United States. [‡]Present address: Components Research, Intel Corporation, Hillsboro, OR 97124. [†]These authors contributed equally to this work.

ABSTRACT

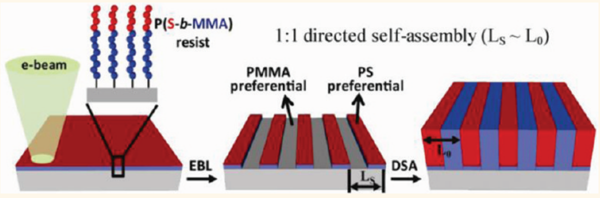

We demonstrate a direct e-beam patternable one-component block copolymer (BCP) resist to fabricate a chemical pattern for the directed assembly of a symmetric block copolymer. The resist consists of a low molecular weight poly(styrene-*block*-methyl methacrylate) with a hydroxyl group at the PMMA chain end (PS-*b*-PMMA-OH), which anchors the chains to the surface. This short-tethered PMMA block provided sufficient sensitivity to allow scission by e-beam. The length of the untethered PS block was fine-tuned to impart the required contrast between the patterned and the unpatterned region for 1:1 assembly of an overlying BCP blend. Two BCP resists with a PS fraction of 0.25 (16SM) and 0.34 (18SM), with a total molecular weight less than 20K, were synthesized, and the assembly of a ternary BCP blend was studied. 16SM- and 18SM-anchored substrates showed nonpreferential and PS preferential surfaces, respectively. Both 18SM and 16SM could be patterned by e-beam to fabricate a 1:1 chemical pattern with a line pitch of 70 nm for the assembly of a BCP ternary blend. 18SM gave fewer defects than 16SM due to an increased contrast in interfacial energies between adjacent stripes in the chemical surface pattern. Two additional PS-*b*-PMMA-OH polymers with a molecular weight of 39K ($F_{PS} = 0.76$) and 69K ($F_{PS} = 0.83$) were synthesized to study the effect of PS cross-linking upon exposure to e-beam. As the PS fraction increases, the line pattern becomes blurred and ultimately ineffective in guiding the BCP assembly. The blurring is attributed to cross-linking of adjacent PS chains.

KEYWORDS: block copolymer · brush · directed assembly · preferential surface · e-beam patterning

Self-assembly of block copolymers (BCPs) in thin film provides a large-area, high-throughput route to creating dense nanostructures in length scales not easily achievable by traditional lithography processes.[1,2] Directed assembly of BCPs on a chemically or topographically patterned surface allows precise registration of features, with the underlying substrate providing resolution enhancement and reducing the number of defects in the assembled structure.[3,4] Nealey and coworkers pioneered the implementation of lithography processes to generate chemical patterns on a substrate for directed assembly of BCPs.[5−7] The schematic in Figure 1a illustrates the current process used to fabricate a chemically nanopatterned surface that subsequently directs the assembly of BCP or BCP blend (a mixture of BCP and the two corresponding homopolymers). A typical process involves spin-coating a photoresist on a polystyrene (PS) brush grafted silicon substrate followed by patterning using advanced lithography (EUV interference or e-beam lithography) to produce line and dot arrays. Oxygen plasma etching is used to chemically modify the exposed regions of the PS brush and convert the topographic photoresist pattern into a chemical surface pattern. During this step, the plasma-treated brush area becomes polar and hydrophilic [poly(methyl methacrylate) (PMMA) preferential], while the unexposed area remains nonpolar and hydrophobic (PS preferential). The resulting chemical pattern can direct the assembly of a BCP or BCP blend to induce dense periodic structures as well as non-regular structures that may allow fabrication of nanoelectronic devices that require patterns more complex than simple periodic arrays.[5,7] The advantages of using BCP to fabricate nanostructures instead of the patterned photoresist itself is the "self-healing" nature[5,7] of the BCP assembly that rectifies the defects in the resist pattern, as well as the ability to use a sparse chemical pattern to multiply the density of features using a suitable BCP.[6,8] For example, Ruiz *et al.*[6] demonstrated that a sparse chemical spot pattern can direct the assembly of cylinder-forming PS-*b*-PMMA that interpolates additional cylinders between the pre-patterned spots, hence resolution enhancement can be achieved while maintaining perfect registration. It has also been shown that spot size

* Address correspondence to pgopalan@cae.wisc.edu.

Received for review December 20, 2011 and accepted January 14, 2012.

10.1021/nn204995z

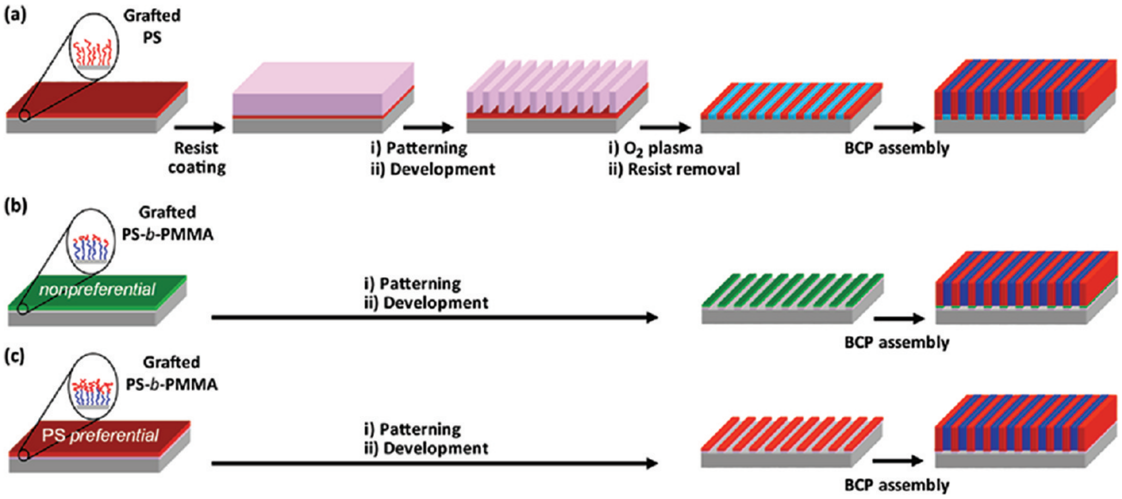

Figure 1. Schematic illustration of (a) the traditional approach for fabricating chemical patterns on PS-anchored surface and our approach of direct patterning of e-beam sensitive nonpreferential (b) and PS preferential (c) block copolymer grafted surfaces.

larger than the cylinder diameter can be used, as the BCP rectifies the pattern to form regularly sized spots with its natural domain spacing. Cheng *et al.* demonstrated a similar result for a lamellae-forming PS-*b*-PMMA.[8]

The two main components involved in creating the chemical pattern for the assembly of PS-*b*-PMMA are (i) a surface-anchored polymer (*e.g.*, PS or PS-*r*-PMMA) that defines the inherent wetting characteristics (preferential or nonpreferential) of the surface toward the overlying BCP film, and (ii) a photoresist (*e.g.*, PMMA) to pattern the surface-anchored polymer. Recently, we demonstrated that the role of these two organic layers (patternability and controlled wettability) can be combined into a one-component system consisting of a surface-anchored BCP-based resist.[9] Photocleavable junction point or a short PMMA segment between the two blocks has been previously used to fabricate functional nanostructures.[10−12] We utilized a surface grafted PS-*b*-PMMA-OH as a direct patternable nonpreferential layer, as the PMMA block provides e-beam sensitivity comparable to traditional resists, and the length of the PS block can be tuned to alter the overall nonpreferentiality of the surface. We further demonstrated that the resist layer can be directly patterned by e-beam to spatially control the domain orientation in the overlying film at submicrometer length scale. The overall molecular weight of the anchored BCP as well as the relative lengths of the two blocks is critical to successful implementation of this one-step approach. In our previous study,[9] the periodicity of the patterned BCP resist or the resulting chemical guiding stripes (L_s) was much larger than the natural periodicity of the BCP (L_0). Patterning the buffer layer (200 nm line width) induced clear alternation in the domain orientation in the overlying BCP film from perpendicular to parallel. However, within the 200 nm line width, the grains were randomly oriented, resulting in poor lateral ordering of the domains. In principle, we can tune the boundary conditions further for assembly by tailoring the composition of the BCP resist and the periodicity of the guiding stripe, hence pushing the limits of this approach to nanometer scale features. Here, we report the first demonstration of directed assembly of BCP ternary blend on a 1:1 chemical pattern [$L_s \sim L_0$] (Figure 1b,c) created using a surface-anchored block copolymer resist. Surface grafted PS-*b*-PMMA-OH was used as an e-beam resist with desired surface wetting properties (either nonpreferential or PS preferential) for fabrication of chemical patterns. The composition and the molecular weight of the BCP resist were optimized for the directed assembly of a BCP ternary blend. The direct patterning approach avoids the undesirable resist effects on the wetting behavior of the underlying brush and also reduces the number of steps involved in the fabrication of chemical patterns by conventional lithography.

RESULTS AND DISCUSSION

Composition of the Surface Grafted Resist. Atom transfer radical polymerization (ATRP) was utilized to synthesize PS-*b*-PMMA-OH (Figure 2a) as reported earlier.[9] The synthesized polymers were thermally grafted on silicon oxide surface to create modified substrates. The molecular weights of the hydroxyl-terminated BCPs were 16K and 18K (Table 1). Henceforth, these two BCPs will be referred to as **16SM** ($F_{PS} = 0.25$) and **18SM** ($F_{PS} = 0.34$), respectively. Macroscopic wetting properties of the modified surfaces from water contact angle measurements show that the **18SM** surface is hydrophobic, similar to a substrate modified with PS homopolymer, while the **16SM** surface exhibits a contact angle similar to that of a substrate grafted with random copolymer having F_{St} of 0.57−0.63.[9] The surface

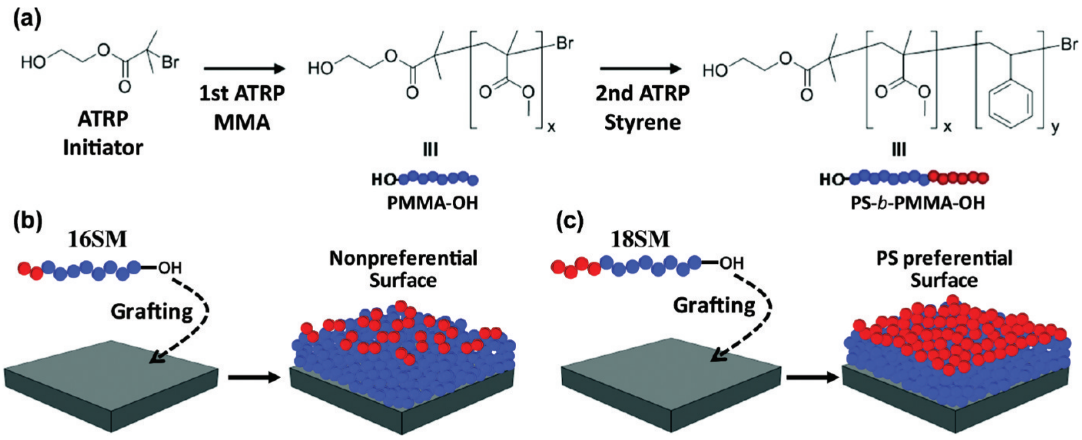

Figure 2. Schematic illustration of the (a) ATRP synthesis of PS-*b*-PMMA-OH and the grafting of the block brush containing varying lengths of the PS block on silicon substrate to fabricate a nonpreferential (b) and PS preferential (c) surface.

TABLE 1. Characteristics of Polymers and Polymer Grafted Surfaces

polymer	M_n (kg/mol)	thickness (nm)	PS fraction (F_{PS})	water contact angle (deg)
PMMA-OH	11500	4.7	0	65
PS-*b*-PMMA-OH (**16SM**)	16200	5.5	0.25	76
PS-*b*-PMMA-OH (**18SM**)	18200	7.5	0.34	86
PS-*b*-PMMA-OH (**39SM**)	39200	11.2	0.76	88
PS-*b*-PMMA-OH (**69SM**)	69100	17.2	0.83	90
PS-OH	6500	4.3	1	88

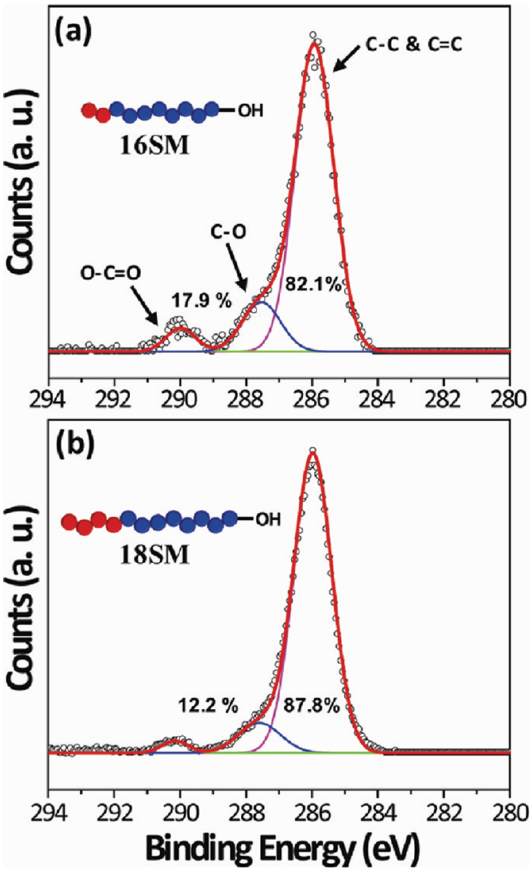

Figure 3. XPS spectra showing multiplex scans of C 1s peak for 16SM (a) and 18SM (b) grafted substrates. Surface chemical compositions were estimated by comparing integrated intensity values of C 1s peaks at 285.8, 287.5, and 290.0 eV.

composition of **16SM** and **18SM** grafted surfaces can be estimated with X-ray photoelectron spectroscopy (XPS). Figure 3 shows the C 1s XPS spectra of **16SM** and **18SM** grafted surfaces. Upon deconvulation of the C 1s peak, three different peaks were assigned to C−C or C═C at 285.8 eV, C−O at 287.5 eV, and O−C═O at 290.0 eV.[13,14] The PMMA block in the grafted chains contributes to the peaks corresponding to C−O and O−C═O bonds, whereas both PS and the backbone of PMMA contribute to the peaks corresponding to C−C or C═C at 285.8 eV. By comparing the integrated intensity of C−O/O−C═O peaks and C−C/C═C peaks, we find that the intensity of the C 1s peak at 285.8 eV (assigned to C−C and C═C) from **18SM** (87.8%) is higher than that from **16SM** (82.1%), confirming higher effective styrene content of the **18SM** surface.

The morphology of these anchored BCPs can play an important role in altering the local *versus* global composition of the modified substrate, hence affecting the self-assembly of an overlying BCP film. Earlier reports on surface grafted BCPs have mainly focused on the stimuli-responsive behavior of anchored brushes by selective solvent treatment or their phase separation behavior.[15,16] Similar to the bulk system, phase separation behavior of grafted block copolymers depends on composition of the polymer (f), degree of polymerization (N), and the Flory−Huggins interaction parameter (χ). In addition, the differences in the surface affinity of two blocks and the grafting density of the chains are equally important.[17] Theoretically, four phases are predicted for grafted block copolymers in an equilibrium state: uniform, hexagonal, stripe,

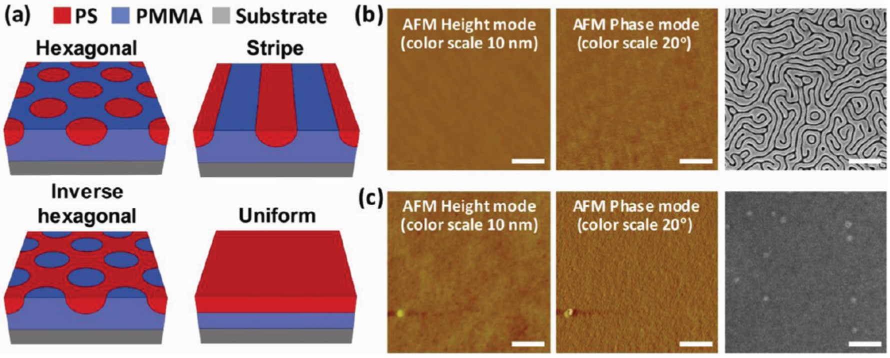

Figure 4. **(a) Theoretically predicted[17] and experimentally verified[18] phases of surface-tethered block copolymers and AFM images of the 16SM (b) and 18SM (c) grafted surfaces showing no discernible phase separation along with the corresponding top view SEM images of assembled lamella-forming ternary blend on block copolymer grafted substrates (AFM images: 1 μm × 1 μm, scale bar = 200 nm; SEM images: 2 μm × 2 μm, scale bar = 400 nm).**

and inverse hexagonal (Figure 4a).[17] Recently, O'Driscoll *et al.* reported a detailed experimental study on the lateral phase separation of surface grafted PS-*b*-PMMA after either thermal or solvent annealing.[18] They investigated the effect of molecular weight and composition of tethered PS-*b*-PMMA on the phase separation behavior. As the composition of the upper PS block (untethered) fraction increases from 0.10 to 0.45, surface morphology changes from disordered (f = 0.10) to hexagonal (f = 0.19−0.24) and inverted hexagonal (f = 0.45), which is qualitatively consistent with the theoretical prediction.[17]

However, for our intended application, phase separation in the lateral direction, for example, hexagonal, stripe, and inverse hexagonal morphology, is not desirable as it might affect the local surface composition and hence pattern quality during directed BCP assembly. To avoid phase separation of grafted PS-*b*-PMMA, we controlled the total molecular weight to be below 20K.[18,19] As a result, the BCP grafted surfaces did not show any discernible phase separation even after thermal annealing (Figure 4b,c).

Evaluation of Nonpreferentiality of the Resist and Direct E-Beam Patterning. Thin film assembly of BCP ternary blend (PS-*b*-PMMA (52K-52K)/PS (49K)/PMMA (50K) (0.7/0.15/0.15 wt%) on PS-*b*-PMMA-OH grafted substrates was examined by SEM. A typical fingerprint pattern generated by vertical lamellae (Figure 4b), and the featureless hole/island surface generated by parallel lamellae (Figure 4c) confirms nonpreferential and preferential wetting conditions for **16SM** and **18SM**, respectively. Fast Fourier transform (FFT) of the fingerprint pattern on nonpreferential **16SM** gave a 70 nm domain spacing (L_0). A 1:1 chemical pattern, that is, a guiding stripe with a periodicity L_s of 70 nm, can be easily fabricated by conventional e-beam lithography. Grafted BCP resist substrate was subjected to direct electron-beam lithography (EBL) to fabricate a chemical pattern for the directed assembly of a BCP ternary blend (Figure 1b,c). Figure 5a,b shows the AFM height images of a line array resulting from the patterned BCP resist, with a 70 nm pitch. As a comparison, a traditional PMMA resist was patterned on a PS grafted substrate following the procedure illustrated in Figure 1a. Figure 5c shows the AFM image of the patterned PMMA resist after development. The required e-beam line dose to create clear line patterns was 0.12−0.6 nC/cm for grafted BCP, which is lower than that for the PMMA resist of 0.4−1 nC/cm.

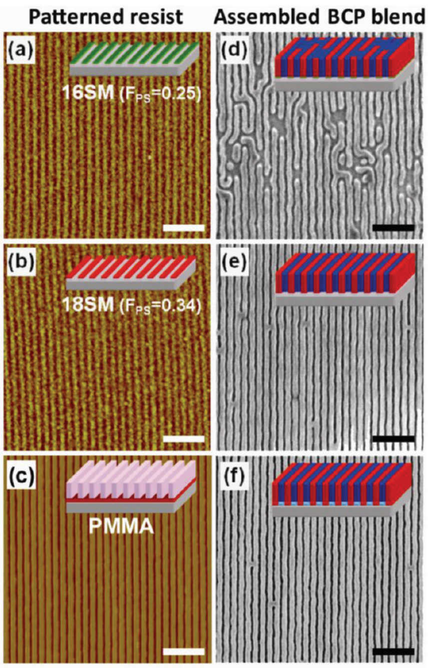

Figure 5. **AFM height mode images of e-beam patterned (70 nm L_S) 16SM (a), 18SM (b), and PMMA resist on a PS grafted substrate (c). Top view SEM images of assembled ternary blends on the corresponding chemical patterns shown in panels a−c are presented in panels d−f (all images: 2 μm × 2 μm, scale bar = 400 nm). (Note: after e-beam patterning of the PMMA resist, underlying grafted PS was exposed to oxygen plasma to create chemical pattern.)**

Figure 5d−f shows the assembled BCP ternary blend on chemically patterned surfaces. The chemical pattern created from **18SM** (F_{PS} = 0.34) showed directed assembly with a small number of defects (Figure 5e)

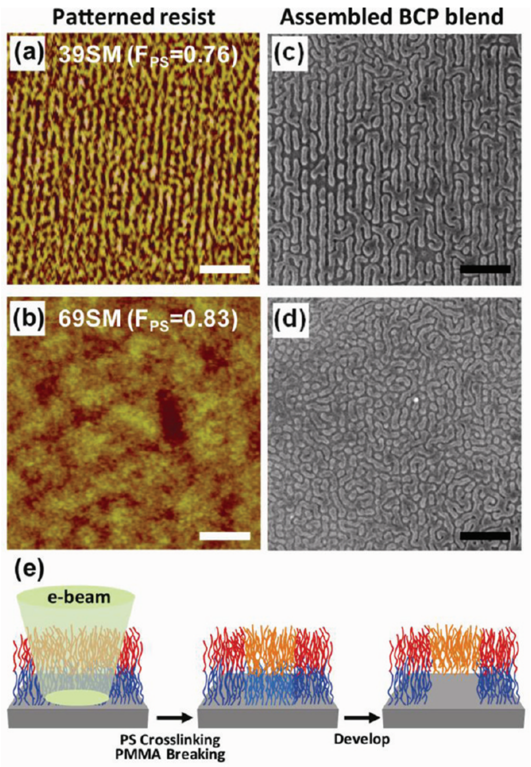

Figure 6. AFM height mode images of e-beam patterned 39SM (a) and 69SM (b), showing increased blurring of the pattern with increasing molecular weight, and (c–d) the corresponding top view SEM images of the assembled ternary blend on the substrates (a) and (b). A schematic illustration of the PS cross-linking induced by e-beam exposure is shown in Figure 5e (all images: 2 μm × 2 μm, scale bar = 400 nm).

comparable to those obtained by patterning a grafted PS brush with a PMMA resist (Figure 5f), whereas assembly on the chemical pattern from a **16SM** (F_{PS} = 0.25) resist was poor. The defect density in the assembled structure is a strong function of the chemical contrast between the guiding stripe and the background of the pattern.[20] In a seminal work, Edwards *et al.*[20] found that interfacial interactions between the blocks of an overlying BCP film and the chemically patterned surface play a critical role in the epitaxial assembly. By increasing the contrast in interfacial energy between adjacent stripes in the chemical surface pattern, perfect epitaxial assembly was achieved with a wide process latitude. In other words, perfect registration cannot be achieved even on a well-defined 1:1 chemical pattern if chemical contrast is not high enough. The chemical pattern fabricated by direct EBL of the anchored BCPs results in a PMMA preferential guiding stripe in both cases, while the background is nonpreferential for **16SM** and PS preferential for **18SM**. The larger chemical contrast in the chemical pattern generated by **18SM** leads to fewer defects in the assembled BCP. Hence, our results confirm that, in fact, these basic assembly rules are still followed with the direct EBL patternable BCP resists, while the processing is tremendously simplified.

For the **18SM** BCP resist, a line dose of 0.33 to 0.48 nC/cm resulted in directed assembly while the PMMA resist required a line dose of 0.68 to 0.89 nC/cm. The difference in dose range between grafted PS-*b*-PMMA-OH and the PMMA resist can be attributed to (i) the molecular weight of the PMMA segment, and (ii) the thickness of the PMMA layer. The lower molecular weight (11K) and thinner layer (~4 nm) of the PMMA block in a grafted PS-*b*-PMMA-OH predictably leads to higher sensitivity toward e-beam compared to the traditional PMMA resist. Thus, by using surface grafted BCP resist, the e-beam writing process can be accomplished in a shorter time.

While we created a chemical pattern from surface grafted PS-*b*-PMMA-OH by virtue of PMMA chain scission, it is known that PS undergoes cross-linking by e-beam exposure, leading to its use as a negative tone e-beam resist.[21] Paik *et al.* demonstrated the fabrication of nanochannels by patterning a PS-*b*-PMMA brush using a negative tone upper block (PS) and a positive tone lower block (PMMA).[22] Compared to our "grafting to" method, Paik *et al.* prepared PS-*b*-PMMA brushes by sequential surface initiated polymerization ("grafting from method"), resulting in much thicker and denser layers of PMMA (30 nm thick) and PS (30–90 nm thick). Hence, most likely, the PS chains cross-link with neighboring PS segments, resulting in the formation of a PS roof layer. We did not observe PS cross-linking by e-beam patterning of **16SM** and **18SM**, probably due to the low total molecular weights (16–18 kg/mol) and the low PS fraction (F_{PS} = 0.25–0.34) in the grafted BCP resist. Furthermore, since the molecular weight of the chains in our study is below the phase segregation limit, the short PS patches (PS block is 4–6 kg/mol) are most likely mixed with the PMMA block, further preventing the cross-linking of PS.

To understand the effect of PS fraction (or chain length) on its cross-linking behavior and hence the quality of resulting chemical pattern, we increased the chain length of PS while keeping the molecular weight of PMMA the same. We prepared two additional PS-*b*-PMMA-OH polymers with molecular weights of 39K (**39SM**, F_{PS} = 0.76) and 69K (**69SM**, F_{PS} = 0.83) and carried out EBL using the same conditions used earlier. The results clearly show that as the PS fraction increases the line pattern becomes blurred (Figure 6a,b) and ultimately ineffective in guiding the BCP assembly (Figure 6c,d). Therefore, controlling the molecular weight and composition of block copolymer based resist is critical to creating well-defined chemical patterns for the directed assembly of BCP or BCP blend.

CONCLUSIONS

In conclusion, we have demonstrated the use of a single-component e-beam resist to create a 1:1 chemical pattern for directed assembly of block copolymers. The resist consists of a surface grafted PS-*b*-PMMA.

Since PS and PMMA can be used as a negative and positive tone e-beam resist, respectively, controlling the relative lengths of the two blocks and the overall molecular weight is critical for directed assembly of BCPs. The BCP resist has a molecular weight below 20K and PS fraction of 0.34 which suppresses phase segregation of the domains and creates a PS preferential substrate. The PMMA block provides the required sensitivity to allow scission by e-beam, resulting in a chemical pattern with sufficient contrast to allow directed assembly of a ternary blend of BCP with its corresponding homopolymers. For creating chemical patterns to direct BCP assembly, in addition to the periodicity of the pattern, the surface wetting characteristics need to be fine-tuned. Recently, Liu *et al.*[23,24] and Cheng *et al.*[25] developed new processes to avoid the wetting alteration problem of surface neutralizing layers, stemming from interactions with an overlying photoresist. In both examples, carefully tuned surface neutralizing materials were anchored to the substrate after the lithographic processes to prevent neutrality alteration. The direct EBL patterning of surface modifying layers that we have presented here avoids contact with the photoresist (PMMA), photogenerated acid, and developer solution and hence offers a more predictable control over the chemical contrast in the chemical pattern. Here, we have demonstrated a pattern with $L_s \sim L_0$, but in principle, creating a sparse chemical pattern for density multiplication is possible using the same approach. The understanding on the patterning of surface grafted BCPs developed in this work can be adapted to areas other than BCP lithography such as sensors, microfluidic devices, and biodiagnostics by selecting an appropriate upper block.

METHODS

Materials. Styrene and methyl methacrylate were purchased from Aldrich and distilled under reduced pressure. Hydroxyl-containing ATRP initiator was synthesized according to the literature.[26] Hydroxyl-terminated PS-*b*-PMMA block copoly mers and homopolymers were synthesized *via* ATRP.[9] BCPs for directed assembly study were purchased from Polymer Source Inc. and used without further purification: symmetric PS-*b*-PMMA (PS 52 kg/mol, PMMA 52 kg/mol), PS homopolymer (49 kg/mol), and PMMA homopolymer (50 kg/mol). PMMA resist (950PMMA-C2) was purchased from Microchem Corp.

Surface Modification and BCP Deposition. Solutions of hydroxyl-terminated PS-*b*-PMMA or hydroxyl-terminated PS in toluene (1% w/w) were spin-coated at 2000 rpm onto precleaned silicon wafers by Piranha solution treatment and then annealed under vacuum at 160 °C for 2 days. The substrates were sonicated in toluene to remove ungrafted block copolymer and rinsed with fresh toluene. On unpatterned or e-beam-patterned BCP grafted wafers, ternary blend solution of PS-*b*-PMMA (52K-52K)/PS (49K)/PMMA (50K) in toluene (0.7/0.15/0.15, total 1% w/w) was spin-coated at 4000 rpm to produce films with thickness of ~30 nm. Spin-coated BCP films were annealed at 220 °C for 24 h under vacuum for the equilibrium morphology prior to imaging.

Characterization. For each synthesized polymer, a ^{1}H NMR spectrum was recorded in solution ($CDCl_3$) with a Bruker AC+ 300 (300 MHz) spectrometer. Molecular weight of polymers was measured with GPC. THF was used as an eluent, and monodisperse polystyrene standards were used for calibration. The film thicknesses of the brush and BCP layers were measured by ellipsometry (Rudolph Research Auto EL). Static contact angles of sessile drops were measured to characterize the hydrophobicity of the surface layers with a Dataphysics OCA 15 Plus goniometer. XPS spectra of BCP grafted surfaces were acquired with a Perkin-Elmer 5400 ESCA spectrometer under Mg Kα X-ray emission. Top-down scanning electron microscope (SEM) images of the BCP microdomains were acquired with a LEO-1550 VP field-emission SEM using an accelerating voltage of 1 kV. The surface topography of BCP resists and PMMA resist was examined using a Nanoscope III Multimode atomic force microscope (Digital Instruments) in tapping mode.

E-Beam Patterning. The electron-beam lithography was performed on BCP grafted substrates and 40 nm of PMMA resist/PS grafted substrate with a LEO 1550-VP field-emission scanning electron microscope (SEM) operating with a J.C. Nabity pattern generation system. The exposure used an accelerating voltage of 20 kV, a beam current of 30 pA, and line doses varied from 0.12 to 0.6 nC/cm for grafted BCP resists and from 0.4 to 1 nC/cm for PMMA resist. Typical e-beam-patterned area was 50 μm × 10 μm. For e-beam-exposed BCP resists, development was done by immersing the patterned substrate in THF for 60 s, followed by rinsing fresh THF and drying. E-beam-patterned PMMA resist was developed by soaking in IPA/MIBK (1/3, v/v) for 30 s, followed by rinsing IPA and drying. After subsequent oxygen plasma treatment and removal of residual PMMA resist, the sample was used for BCP directed assembly.

Conflict of Interest: The authors declare no competing financial interest.

Acknowledgment. We acknowledge support from staff and the use of equipment at the Center for Nanotechnology and the Synchrotron Radiation Center at the University of Wisconsin (National Science Foundation Grant No. DMR-0537588). This research was funded by the National Science Foundation-Nanoscale Science and Engineering Center at the University of Wisconsin—Madison (Grant No. DMR-0832760).

Note Added after ASAP Publication: This manuscript was published ASAP on January 24, 2012. The title was modified and the revised version was published on February 8, 2012.

REFERENCES AND NOTES

1. Hawker, C. J.; Russell, T. P. Block Copolymer Lithography: Merging "Bottom-Up" with "Top-Down" Processes. *MRS Bull.* **2005**, *30*, 952–966.
2. Segalman, R. A. Patterning with Block Copolymer Thin Films. *Mater. Sci. Eng., R* **2005**, *48*, 191–226.
3. Bita, I.; Yang, J. K. W.; Jung, Y. S.; Ross, C. A.; Thomas, E. L.; Berggren, K. K. Graphoepitaxy of Self-Assembled Block Copolymers on Two-Dimensional Periodic Patterned Templates. *Science* **2008**, *321*, 939–943.
4. Cheng, J. Y.; Ross, C. A.; Smith, H. I.; Thomas, E. L. Templated Self-Assembly of Block Copolymers: Top-Down Helps Bottom-Up. *Adv. Mater.* **2006**, *18*, 2505–2521.
5. Kim, S. O.; Solak, H. H.; Stoykovich, M. P.; Ferrier, N. J.; de Pablo, J. J.; Nealey, P. F. Epitaxial Self-Assembly of Block Copolymers on Lithographically Defined Nanopatterned Substrates. *Nature* **2003**, *424*, 411–414.
6. Ruiz, R.; Kang, H.; Detcheverry, F. A.; Dobisz, E.; Kercher, D. S.; Albrecht, T. R.; de Pablo, J. J.; Nealey, P. F. Density Multiplication and Improved Lithography by Directed Block Copolymer Assembly. *Science* **2008**, *321*, 936–939.
7. Stoykovich, M. P.; Müller, M.; Kim, S. O.; Solak, H. H.; Edwards, E. W.; de Pablo, J. J.; Nealey, P. F. Directed Assembly of Block Copolymer Blends into Nonregular Device-Oriented Structures. *Science* **2005**, *308*, 1442–1446.

8. Cheng, J. Y.; Rettner, C. T.; Sanders, D. P.; Kim, H.-C.; Hinsberg, W. D. Dense Self-Assembly on Sparse Chemical Patterns: Rectifying and Multiplying Lithographic Patterns Using Block Copolymers. *Adv. Mater.* **2008**, *20*, 3155–3158.
9. Han, E.; Leolukman, M.; Kim, M.; Gopalan, P. Resist Free Patterning of Nonpreferential Buffer Layers for Block Copolymer Lithography. *ACS Nano* **2010**, *4*, 6527–6534.
10. Bang, J.; Kim, S. H.; Drockenmuller, E.; Misner, M. J.; Russell, T. P.; Hawker, C. J. Defect-Free Nanoporous Thin Films from ABC Triblock Copolymers. *J. Am. Chem. Soc.* **2006**, *128*, 7622–7629.
11. Goldbach, J. T.; Russell, T. P.; Penelle, J. Synthesis and Thin Film Characterization of Poly(styrene-*block*-methyl methacrylate) Containing an Anthracene Dimer Photocleavable Junction Point. *Macromolecules* **2002**, *35*, 4271–4276.
12. Ryu, J.-H.; Park, S.; Kim, B.; Klaikherd, A.; Russell, T. P.; Thayumanavan, S. Highly Ordered Gold Nanotubes Using Thiols at a Cleavable Block Copolymer Interface. *J. Am. Chem. Soc.* **2009**, *131*, 9870–9871.
13. Ton-That, C.; Campbell, P. A.; Bradley, R. H. Frictional Force Microscopy of Oxidized Polystyrene Surfaces Measured Using Chemically Modified Probe Tips. *Langmuir* **2000**, *16*, 5054–5058.
14. Yu, W. H.; Kang, E. T.; Neoh, K. G. Controlled Grafting of Well-Defined Polymers on Hydrogen-Terminated Silicon Substrates by Surface-Initiated Atom Transfer Radical Polymerization. *J. Phys. Chem. B* **2003**, *107*, 10198–10205.
15. Zhao, B.; Brittain, W. J.; Zhou, W.; Cheng, S. Z. D. Nanopattern Formation from Tethered PS-*b*-PMMA Brushes upon Treatment with Selective Solvents. *J. Am. Chem. Soc.* **2000**, *122*, 2407–2408.
16. Zhao, B.; Brittain, W. J.; Zhou, W.; Cheng, S. Z. D. AFM Study of Tethered Polystyrene-*b*-Poly(methyl methacrylate) and Polystyrene-*b*-Poly(methyl acrylate) Brushes on Flat Silicate Substrates. *Macromolecules* **2000**, *33*, 8821–8827.
17. Matsen, M. W.; Griffiths, G. H. Melt Brushes of Diblock Copolymer. *Eur. Phys. J. E* **2009**, *29*, 219–227.
18. O'Driscoll, B. M. D.; Griffiths, G. H.; Matsen, M. W.; Perrier, S.; Ladmiral, V.; Hamley, I. W. Lateral Phase Separation in Grafted Diblock Copolymer Films. *Macromolecules* **2010**, *43*, 8177–8184.
19. Bates, F. S.; Fredrickson, G. H. Block Copolymer Thermodynamics: Theory and Experiment. *Annu. Rev. Phys. Chem.* **1990**, *41*, 525–557.
20. Edwards, E. W.; Montague, M. F.; Solak, H. H.; Hawker, C. J.; Nealey, P. F. Precise Control over Molecular Dimensions of Block-Copolymer Domains Using the Interfacial Energy of Chemically Nanopatterned Substrates. *Adv. Mater.* **2004**, *16*, 1315–1319.
21. Austin, M. D.; Zhang, W.; Ge, H.; Wasserman, D.; Lyon, S. A.; Chou, S. Y. 6 nm Half-Pitch Lines and 0.04 μm^2 Static Random Access Memory Patterns by Nanoimprint Lithography. *Nanotechnology* **2005**, *16*, 1058–1061.
22. Paik, M. Y.; Xu, Y.; Rastogi, A.; Tanaka, M.; Yi, Y.; Ober, C. K. Patterning of Polymer Brushes. A Direct Approach to Complex, Sub-surface Structures. *Nano Lett.* **2010**, *10*, 3873–3879.
23. Liu, C.-C.; Han, E.; Onses, M. S.; Thode, C. J.; Ji, S.; Gopalan, P.; Nealey, P. F. Fabrication of Lithographically Defined Chemically Patterned Polymer Brushes and Mats. *Macromolecules* **2011**, *44*, 1876–1885.
24. Liu, C.-C.; Nealey, P. F.; Raub, A. K.; Hakeem, P. J.; Brueck, S. R. J.; Han, E.; Gopalan, P. Integration of Block Copolymer Directed Assembly with 193 Immersion Lithography. *J. Vac. Sci. Technol., B* **2010**, *28*, C6B30–C6B34.
25. Cheng, J. Y.; Sanders, D. P.; Truong, H. D.; Harrer, S.; Friz, A.; Holmes, S.; Colburn, M.; Hinsberg, W. D. Simple and Versatile Methods To Integrate Directed Self-Assembly with Optical Lithography Using a Polarity-Switched Photoresist. *ACS Nano* **2010**, *4*, 4815–4823.
26. Jakubowski, W.; Lutz, J.-F.; Slomkowski, S.; Matyjaszewski, K. Block and Random Copolymers as Surfactants for Dispersion Polymerization. I. Synthesis *via* Atom Transfer Radical Polymerization and Ring-Opening Polymerization. *J. Polym. Sci., Part A: Polym. Chem* **2005**, *43*, 1498–1510.